

# PHOTOMASK

BACUS—The international technical group of SPIE dedicated to the advancement of photomask technology.

BACUS

N • E • W • S

JUNE 2020  
VOLUME 36, ISSUE 6

PUV20 - 2nd Place Winner Best Student Poster

## Alkyltin Keggin clusters as EUVL photoresist technology

**Rebecca D. Stern**, Department of Materials Science and Engineering, University of California Berkeley, Berkeley, CA, 94720

**Danielle C. Hutchison, Morgan R. Olsen, and May Nyman**, Department of Chemistry, Oregon State University, Corvallis, OR, 97331, USA

**Lev N. Zakharov**, Department of Chemistry and Biochemistry, University of Oregon, Eugene, OR, 97403, USA

**Kristin A. Persson**, Department of Materials Science and Engineering, University of California Berkeley, Berkeley, Lawrence Berkeley National Laboratory, Berkeley, CA, 94720, USA

### ABSTRACT

Extreme ultraviolet lithography is the newest technique to keep up with Moore's law and create smaller integrated circuit feature sizes. However, novel photoresist materials must be used in order to withstand the high energy beam ( $\lambda=13.5\text{nm}$ ). Metal-oxo clusters have been proposed as one photoresist solution, and specifically the most promising is a sodium-centered tin-Keggin cluster. A simple one-step synthesis was developed to produce a Na-Sn Keggin cluster, without the need for heating, filtration, or recrystallization. However, the product was a mixture of the  $\beta$ -isomer ( $\beta\text{-NaSn}_{12}$ ) and the  $\gamma$ -isomer ( $\gamma\text{-NaSn}_{12}$ ), which share the formula  $[(\text{MeSn})_{12}(\text{NaO}_4)(\text{OCH}_2)_{12}(\text{O})_4(\text{OH})_8]^{1+}$ . For fundamental studies on the lithographic mechanisms occurring during exposure to be successful, a pure and stable isomer is desired. Computational modeling was recruited to determine the ground state energy of all five uncapped isomers in this Na-Sn Keggin system. Additionally, the inclusion of one or two tin atoms to the uncapped structure, called capping, altered which isomers were stabilized. Computations were also employed to evaluate the influence of this capping strategy for the single-capped  $\beta$ -isomer ( $\beta\text{-NaSn}_{13}$ ), the single-capped  $\alpha$ -isomer ( $\alpha\text{-NaSn}_{13}$ ), the single-capped  $\gamma$ -isomer ( $\gamma\text{-NaSn}_{13}$ ), and the double-capped  $\gamma$ -isomer ( $\gamma\text{-NaSn}_{14}$ ). Density functional theory (DFT) was used to obtain the hydrolysis Gibbs free energy and HOMO-LUMO gap, which led to the stability ranking:  $\beta\text{-NaSn}_{12} > \gamma\text{-NaSn}_{12} > \alpha\text{-NaSn}_{12} > \delta\text{-NaSn}_{12} > \epsilon\text{-NaSn}_{12}$  for uncapped clusters, which was consistent with experimental observations. The uncapped isomers were computationally evaluated to be more stable than their respective single-capped analogues. However, the double-capped  $\gamma\text{-NaSn}_{14}$  was more stable than either the uncapped or single-capped clusters. Therefore, capping has shown to be a useful tool in exploring the stability landscape of these Keggin clusters to promote a pure and stable material for the next generation EUV lithography photoresists. And noteworthy, this sodium-centered tin-Keggin ion represents the only Keggin ion family so far, that favors the isomers of lower symmetry.

### 1. Introduction

With integrated circuit manufacturers aiming to produce sub-10nm feature sizes, extreme ultraviolet lithography (EUVL) is perceived as the next developing technology, at a wavelength of only 13.5nm.<sup>1</sup> The challenges

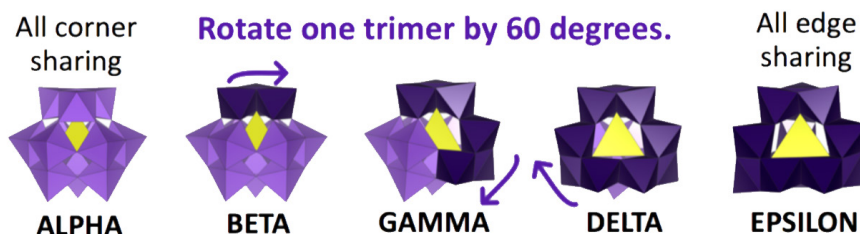


Figure 1. Trimer rotation to obtain five Keggin isomers  $\alpha$ ,  $\beta$ ,  $\gamma$ ,  $\delta$ , and  $\epsilon$ .

TAKE A LOOK  
INSIDE:

INDUSTRY BRIEFS  
—see page 7

CALENDAR  
For a list of meetings  
—see page 8

SPIE.

# EDITORIAL

## COVID-19 and Communication

**Doug Resnick, Canon**

In late February, many of us travelled to San Jose to take part in the SPIE Advanced Lithography Symposium. At the same time, COVID-19 had already impacted China and was moving into other countries in Asia. This ended up affecting SPIE AL in a couple of different ways. First, attendance was down, as folks from Korea, as an example, were restricted from traveling. Second, many social and networking events were either cancelled or reduced in scope. It is easy to take the view, that events such as workshops and receptions have little value and are simply a good way to get a free meal and a few drinks. The reality is that these venues provide a valuable service to our community. They provide an opportunity not only to establish or renew friendships, but to communicate and exchange new ideas with folks that you don't ordinarily get to speak with on a regular basis.

These dialogues are critical to the advancement of our industry. The problems we try to solve on a daily basis in order to enhance our technology are far from simple. It encompasses much more than extending logic to the next node, finding ways to stack even more layers on a NAND Flash device or extending the resolution and overlay capabilities of the next lithography tool. Advancements in artificial intelligence, along with the emergence of newer technologies such as quantum computing and augmented reality will have an impact on society and need to be supported with other tools such as big data analysis and complementary computational methods. The point to me made is that the exchange of ideas with your extended network is critical to the advancement of technology. The problems are too hard to solve without cooperation and collaboration.

Almost immediately following SPIE AL, a couple of other things happened. First, travel to the office was restricted and many of us started working from home and have continued to work from home. This new way of working immersed us into the world of Skype calls and Microsoft Teams in order to continue our communications. But the transition was not always seamless, as we struggled with issues such as poor WIFI connections, dropped connections, barking dogs, bad violin lessons in the background and so on. For myself, I have given many impassioned speeches during a Skype meeting, only to realize that my microphone was muted (admit, you've done it too). But we continue to get better at communicating in this way, even though it is far from perfect.

The second thing that occurred was restricted travel in general. This meant no visits to customers and partners, and cancellations of conferences that we rely on for information and networking. Many conferences are beginning to restart, but the venues are digital (online) in form. This is a big step forward, in that we still get to hear about the latest innovations. But what is missing are the networking opportunities. It is likely that for the foreseeable future, digital presentations will be required. Let's find ways to make these forums more interactive. The exchange of ideas is critical to our future and these exchanges require a new way of interacting.

So until we can all safely meet again in person, I invite you for a virtual drink and the opportunity to meet online to discuss new ideas. Stay safe.



N • E • W • S

BACUS News is published monthly by SPIE for BACUS, the international technical group of SPIE dedicated to the advancement of photomask technology.

**Managing Editor/Graphics** Linda DeLano

**SPIE Sales Representative, Exhibitions, and Sponsorships**  
Melissa Valum

**BACUS Technical Group Manager** Marilyn Gorsuch

### ■ 2020 BACUS Steering Committee ■

#### President

**Peter D. Buck**, *Mentor Graphics Corp.*

#### Vice-President

**Emily E. Gallagher**, *imec*

#### Secretary

**Kent Nakagawa**, *Toppa Photomasks, Inc.*

#### Newsletter Editor

**Artur Balasinski**, *Cypress Semiconductor Corp.*

#### 2020 Photomask + Technology Conference Chairs

**Moshe Preil**, *KLA-Tencor Corp.*

**Stephen P. Renwick**, *Nikon Research Corp. of America*

#### International Chair

**Uwe F. W. Behringer**, *UBC Microelectronics*

#### Education Chair

**Frank E. Abboud**, *Intel Corp.*

#### Members at Large

**Michael D. Archuletta**, *RAVE LLC*

**Brian Cha**, *Samsung Electronics Co., Ltd.*

**Derren Dunn**, *IBM Corp.*

**Thomas B. Faure**, *GLOBALFOUNDRIES Inc.*

**Aki Fujimura**, *DS2, Inc.*

**Brian J. Grenon**, *Grenon Consulting*

**Jon Haines**, *Micron Technology Inc.*

**Naoya Hayashi**, *Dai Nippon Printing Co., Ltd.*

**Bryan S. Kasproicz**, *Photronics, Inc.*

**Patrick M. Martin**, *Applied Materials, Inc.*

**Jan Hendrik Peters**, *bmbg consult*

**Jed Rankin**, *GLOBALFOUNDRIES Inc.*

**Douglas J. Resnick**, *Canon Nanotechnologies, Inc.*

**Thomas Scheruebl**, *Carl Zeiss SMT GmbH*

**Thomas Struck**, *Infineon Technologies AG*

**Bala Thumma**, *Synopsys, Inc.*

**Anthony Vacca**, *Automated Visual Inspection*

**Vidya Vaenkatesan**, *ASML Netherlands BV*

**Michael Watt**, *Shin-Etsu MicroSi Inc.*

**Larry Zurbrick**, *Keysight Technologies, Inc.*

## SPIE.

P.O. Box 10, Bellingham, WA 98227-0010 USA

Tel: +1 360 676 3290

Fax: +1 360 647 1445

SPIE.org

help@spie.org

©2020

All rights reserved.

with using polymer-based photoresists for EUVL can be eliminated by using metal-oxo cluster photoresists. Metal-oxo clusters are smaller than the bulky carbon chains in the polymer-based resists, thus preventing pattern collapse. Also, metal-oxo clusters are more durable during the lithographic etching step. Metal-oxo systems previously investigated as potential photoresist materials include hafnium, antimony, and tin clusters.<sup>2-6</sup> These systems have a high EUV atomic absorption cross-section, needed for proper resist functionality.<sup>7</sup> Each system had their limitations however. Hafnium-based clusters demonstrated 8nm resolution but resulted in background condensation.<sup>2</sup> Antimony-oxo clusters had EUV sensitivity but pattern collapse limited high resolution.<sup>3</sup> The tin-oxo “football” cluster prevented background condensation, but the synthesis was difficult.<sup>4</sup> A capped sodium-centered organotin-oxo Keggin cluster produced high aspect ratio and dense line patterns with helium ion beam lithography, but synthesis of the structure was difficult leading to poor reproducibility and low yields.<sup>5,6</sup>

It is thought that the cleavage of the Sn-C bond of the terminal butyl ligands in this material is the cause of the change in the solubility of this photoresist.<sup>8</sup> In order to evaluate this system in more depth, a simplified synthesis strategy was required to further investigate the possibilities of a sodium center organotin-oxo Keggin cluster as a photoresist for EUV lithography. Hutchison and coworkers recently discovered a simple one-step synthesis for the Na-Sn Keggin system that proceeds at room temperature and does not require any filtration or recrystallization.<sup>9</sup> This synthesis strategy successfully made the  $[(\text{MeSn})_{12}(\text{NaO}_4)(\text{OCH}_3)_{12}(\text{O})_4(\text{OH})_8]^{1+}$ , which is an uncapped Keggin cluster denoted  $\beta\text{-NaSn}_{12}$ . However, this synthesis led to a mixture of uncapped  $\beta\text{-NaSn}_{12}$  and uncapped  $\gamma\text{-NaSn}_{12}$  isomers. Computational studies were recruited to investigate this dilemma and unknown cause. Since the Keggin geometry has 5 possible isomers, all 5 uncapped  $\text{NaSn}_{12}$  isomers  $\alpha$ ,  $\beta$ ,  $\gamma$ ,  $\delta$ , and  $\epsilon$ , were computationally modeled in this paper. To evaluate the influence of capping on the prevention of isomerization between uncapped  $\beta\text{-NaSn}_{12}$  and uncapped  $\gamma\text{-NaSn}_{12}$ , the experimentally observed capped  $\beta\text{-NaSn}_{13}$  and  $\gamma\text{-NaSn}_{13}$ , as well as the most recently synthesized double capped  $\gamma\text{-NaSn}_{14}$  were computationally modeled in this paper as well.<sup>9,10</sup> The advantages of using computational modeling tools is to be able to evaluate the thermodynamic stability of experimental as well as theoretical isomers of a given system. The calculated thermodynamic landscape of the isomers enables comparison of the isomer stability and hence interpretation of experimental results. Ideally, computational results will guide synthesis design, being able to determine the influential factors that drive stability between isomers and predict new structures.

## 2. Description of Structures

### 2.1 The Keggin geometry

The Keggin cluster was first structurally characterized in 1934 by J.F. Keggin.<sup>11</sup> It contains a heteroatom metal center in a 4-coordinate environment. Surrounding this are four trimer units. Each trimer unit consists of three metals in a 6-coordinate environment. The three octahedra are edge-sharing within the trimer unit. The  $\alpha$ -isomer is defined as having its four trimer units connected by corner-sharing between trimers, resulting

in Td symmetry, as shown in Figure 1. If one trimer unit is rotated by 60 degrees, the  $\beta$ -isomer is obtained which still exhibits only corner-sharing trimers but with a reduced symmetry of C<sub>3v</sub>. Continuing this process of successive trimer rotations of 60 degrees, the  $\gamma$ -isomer of C<sub>2v</sub> symmetry is obtained. Finally, a rotation of a third trimer yields the  $\delta$ -isomer and a fourth trimer rotation yields the  $\epsilon$ -isomer, possessing C<sub>3v</sub> and Td symmetries, respectively.

### 2.2 Situation I: Mixed $\beta/\gamma\text{-NaSn}_{12}$

The one-step synthesis strategy developed by Hutchison *et al.* occurred at room temperature and did not require any filtration or recrystallization.<sup>9</sup> However, <sup>119</sup>Sn-NMR and single-crystal x-ray diffraction showed a mixture of  $\beta\text{-NaSn}_{12}$  and  $\gamma\text{-NaSn}_{12}$ . To investigate the isomerization, all five uncapped Na-Sn Keggin isomers ( $\alpha$ ,  $\beta$ ,  $\gamma$ ,  $\delta$ ,  $\epsilon$ ) were computationally modeled. They all were given the same formula:  $[(\text{MeSn})_{12}(\text{NaO}_4)(\text{OCH}_3)_{12}(\text{O})_4(\text{OH})_8]^{1+}$ . The  $\beta\text{-NaSn}_{12}$  and  $\gamma\text{-NaSn}_{12}$  clusters are shown in Figure 2a and 2b, respectively. To decrease the computational cost and complexity of these models, the butyl Sn-terminal ligands were replaced with methyl ligands, a common practice.<sup>12</sup> In this Na-Sn Keggin system, the central heteroatom is sodium. Each trimer unit of the Keggin is comprised of three  $\text{MeSnO}_5$  octahedra with a methyl terminal ligand on each tin atom. The three bridging oxygens within each trimer unit (12 total O<sup>2-</sup>) are methoxy ligands. The bridging oxygens between the four trimer units (12 total O<sup>2-</sup>) are oxo or hydroxyl ligands. The overall charge of the structures is determined by the total number of hydroxyl ligands. The location of the hydroxyl ligands impacts the hydrolysis Gibbs free energy and care was taken to obtain the lowest energy conformation. Although the hydrogen location cannot be inferred from the x-ray diffraction data, mass spectrometry identified the overall charge of the structures and bond-valence sum helped guide the hydroxyl ligand placement.

### 2.3 Situation II: Single-capped $\beta\text{-NaSn}_{13}$

Saha *et al.* in 2017 produced a single-capped  $\beta\text{-NaSn}_{13}$ .<sup>5</sup> However, authors found impurities of uncapped  $\text{NaSn}_{12}$  isomers and  $\text{Sn}_{12}$  (i.e. the “football” cluster  $[(\text{RSn})_{12}\text{O}_{14}(\text{OH})_6]^{2+}$ , R=alkyl) co-crystallized with  $\beta\text{-NaSn}_{13}$  in unknown quantities, as determined with electrospray ionization mass spectroscopy (ESI-MS) and <sup>119</sup>Sn-NMR. The computationally modeled  $\beta\text{-NaSn}_{13}$  was assigned a formula of  $[(\text{MeSn})_{12}(\text{NaO}_4)(\text{OCH}_3)_{12}(\text{O})_8(\text{OH})_4(\text{Sn}(\text{H}_2\text{O})_2)]^{1+}$  which is exactly consistent with the experimental crystal structure determined by ESI-MS.<sup>9</sup> The cap position and bonding for theoretical  $\alpha\text{-NaSn}_{13}$  was modeled after  $\beta\text{-NaSn}_{13}$  since these two isomers exhibit similar symmetries and capping “windows” as compared to  $\gamma\text{-NaSn}_{13}$ . The cap on  $\beta\text{-NaSn}_{13}$  and  $\alpha\text{-NaSn}_{13}$  is a 6-coordinate tin, with four bonds to the cluster in the tetragonal window. The two terminal ligands are waters. The single-capped  $\beta\text{-NaSn}_{13}$  is shown in Figure 2c.

### 2.4 Situation III: Single-capped $\gamma\text{-NaSn}_{13}$

A different synthesis strategy conducted by Hutchison *et al.* produced single-capped  $\gamma\text{-NaSn}_{13}$ .<sup>9</sup> However, crystals of both  $\gamma\text{-NaSn}_{13}$  and uncapped  $\beta\text{-NaSn}_{12}$  were isolated from the same closed vial.<sup>9</sup> This computational study modeled the  $\gamma\text{-NaSn}_{13}$  as  $[(\text{MeSn})_{12}(\text{NaO}_4)(\text{OCH}_3)_{12}(\text{O})_6(\text{OH})_6(\text{Sn}(\text{Me}))]$

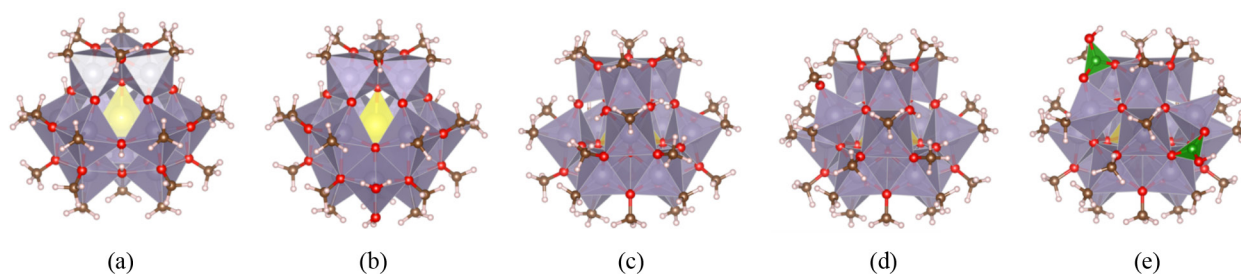


Figure 2. (a) uncapped  $\beta\text{-NaSn}_{12}$  (b) single-capped  $\beta\text{-NaSn}_{13}$  (c) uncapped  $\gamma\text{-NaSn}_{12}$  (d) single-capped  $\gamma\text{-NaSn}_{13}$  (e) double-capped  $\gamma\text{-NaSn}_{14}$ . Tin are purple octahedra, sodium is central yellow tetrahedra, carbon are brown, hydrogen are white, and boron are green.

(OCH<sub>3</sub>)<sub>2</sub>]]<sup>+</sup> as shown in Figure 2d. The cap is a 5-coordinate tin, with three bonds to the cluster in one of the pentagonal windows adjacent to the edge sharing trimer units. The two terminal ligands are methyl and methoxy.

### 2.5 Situation IV: Double-capped $\gamma$ -NaSn<sub>14</sub>

Zhu et al. very recently synthesized the double-capped  $\gamma$ -NaSn<sub>14</sub> in 2019.<sup>10</sup> This synthesis strategy successfully prevented isomerization, yielding pure  $\gamma$ -NaSn<sub>14</sub>. Two 5-coordinate tin caps are found on the structure, one in each pentagonal window on either side of the edge shared between two trimer units. The terminal ligands are a butyl chain (modeled as methyl) and an oxygen atom from a BO<sub>2</sub>(OH) ligand. The two borate ligands provide a bridge between the tin cap and they each replace one methoxy ligand within a trimer unit. The authors believe the borate group stabilizes the cap, which in turn stabilizes the Keggin cluster. This structure is shown in Figure 2e.

## 3. Methodology

### 3.1 Approach

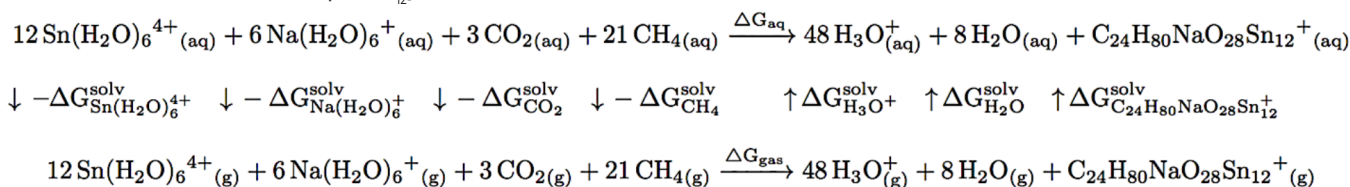
The experimentally isolated clusters were computationally modeled. These consisted of the two uncapped isomers ( $\beta$ -NaSn<sub>12</sub>,  $\gamma$ -NaSn<sub>12</sub>), the two single-capped isomers ( $\beta$ -NaSn<sub>13</sub>,  $\gamma$ -NaSn<sub>13</sub>), and the one double-capped isomer ( $\gamma$ -NaSn<sub>14</sub>). Additionally, theoretical clusters (which have never been experimentally isolated) of the Na-Sn system were also modeled. These included three uncapped isomers ( $\alpha$ -NaSn<sub>12</sub>,  $\delta$ -NaSn<sub>12</sub>,  $\epsilon$ -NaSn<sub>12</sub>), and one single-capped isomer ( $\alpha$ -NaSn<sub>13</sub>), bringing the total number of systems investigated to nine.

We determined the hydrolysis Gibbs free energy ( $\Delta G_{\text{aq}}$ ) in solution by using a thermodynamic cycle in which the hydrolysis energy is the sum of the corresponding gas-phase Gibbs free energy ( $\Delta G_{\text{gas}}$ ) and the Gibbs free energies of solvation  $\Delta G_{\text{sol}}$  as seen in Equation 1. The thermodynamic cycle is used to reduce errors when calculating the solvation energy and comparing structures of different formula.<sup>13-16</sup> The gas-phase Gibbs free energy contains a correction term that takes into account the enthalpy, entropy, and temperature of the system when a frequency analysis is conducted. The term “n” is the coefficient of that species. An example of this thermodynamic cycle using  $\beta$ -NaSn<sub>12</sub> is shown in Scheme 1. The dielectric constant for the solvent model was set to ~78.36, consistent with water.

Scheme 1.

$$\Delta G_{\text{aq}} = \Delta G_{\text{gas}} + \sum_{i=1}^{N_{\text{products}}} n_i \Delta G_i^{\text{sol}} - \sum_{j=1}^{N_{\text{reactants}}} n_j \Delta G_j^{\text{sol}} \quad (1)$$

Scheme 2. Thermodynamic cycle for  $\beta$ -NaSn<sub>12</sub>.



### 3.2 Computational details

The geometry of each cluster was first optimized using Gaussian 09 in the gas phase using the B3LYP functional.<sup>17</sup> The basis set 6-31G(d) was used for elements Na, Ca, C, H, and O, while the basis set LANL2DZ was used for the element Sn.<sup>18,19</sup> A subsequent frequency calculation was performed to verify the absence of imaginary vibration modes to confirm that the system is in a stable/metastable state. An effective core potential LANL2DZ was used for Sn. The geometry was further optimized in water using the continuum solvation model SMD.<sup>20</sup> The electronic energy was refined using a B3LYP single point with the basis set 6-311+G(d,p) for elements Na, Ca, C, H, and O, and basis set LANL2DZ for Sn.<sup>21</sup> The solvation energy was computed using a B3LYP/6-31G(d) single point with SMD for water ( $\epsilon$ ~78.36).

## 4. Results and Discussion

The hydrolysis Gibbs free energy in kcal mol<sup>-1</sup> and HOMO-LUMO gap in eV are listed in Table 1 for each of the nine clusters investigated. The more stable clusters should exhibit a relatively low hydrolysis Gibbs free energy and a relatively large HOMO-LUMO gap. In our case, the stability ordering is evaluated by the hydrolysis Gibbs free energy. The HOMOLUMO gaps are too close in energy to conclusively determine the isomer stability ordering, but rather used to support the results from the Gibbs free energy.

The uniqueness of the tin-oxo Keggin system is that it prefers the less symmetric isomers,  $\beta$  and  $\gamma$ . To our knowledge, no other Keggin cluster systems have been discovered where the  $\beta$  and  $\gamma$  isomers are the most stable. Traditional polyoxometalates like the W- and Mo-Keggin clusters prefer the  $\alpha$  and  $\beta$  isomers.<sup>22</sup> The Al-Keggin and Sb-Keggin favor the  $\epsilon$  isomer.<sup>12,23</sup> And the Cr-Keggin has been recently synthesized as the  $\delta$ -isomer.<sup>24,25</sup> A visual guide for the joint results of the four synthesis strategies (bolded values) and the relevant isomer energy differences are shown in Figure 3. The hydrolysis Gibbs free energy differences between the uncapped clusters are similar in magnitude to previously reported polyoxometalates.<sup>26,27</sup> Synthesis strategy I produced a mixture of uncapped  $\beta$ -NaSn<sub>12</sub> and  $\gamma$ -NaSn<sub>12</sub> clusters, as shown in Figure 3.<sup>9</sup> The calculated relative instability of the uncapped  $\alpha$ -NaSn<sub>12</sub> compared to the uncapped  $\beta$ -NaSn<sub>12</sub> and  $\gamma$ -NaSn<sub>12</sub> is in accordance with our experimental results, such that it has not been experimentally observed.<sup>9</sup> We hypothesize that the reason  $\gamma$ -NaSn<sub>12</sub> is 10 kcal mol<sup>-1</sup> more unstable than  $\beta$ -NaSn<sub>12</sub> is due to the electrostatic repulsion from the Sn-Sn edge-sharing distance being 3.26 Å, while the Sn-Sn corner-sharing distance is ~3.4-3.5 Å.<sup>9</sup>

Synthesis strategy II performed by *Saha et al.* in 2017 produced a charge neutral single-capped  $\beta$ -NaSn<sub>13</sub>.<sup>5</sup> However, authors found impurities of uncapped NaSn<sub>12</sub> and Sn<sub>12</sub> (i.e. the ‘football’ cluster [(RSn)<sub>12</sub>O<sub>14</sub>(OH)<sub>6</sub>]<sup>2+</sup>, R=alkyl) co-crystallized with  $\beta$ -NaSn<sub>13</sub> in unknown quantities, as determined with ESI-MS and <sup>119</sup>Sn-NMR. Results for this situation are shown in Figure 3. The computational results performed in this study indicate that single-capped  $\beta$ -NaSn<sub>13</sub> is more unstable than uncapped  $\beta$ -NaSn<sub>12</sub> by 37.5 kcal mol<sup>-1</sup> and uncapped  $\gamma$ -NaSn<sub>12</sub> by 27.5 kcal mol<sup>-1</sup>. One interpretation of these results is that a hydrolysis Gibbs free energy difference of 37.5 kcal mol<sup>-1</sup> between a capped and uncapped system is not sufficient to prevent the respective uncapped system from forming. We also note that it is possible that specific isomers explicitly interact more strongly

with the solution, which would not be captured in our mean-field solvation approach.

Synthesis strategy III produced single-capped  $\gamma$ -NaSn<sub>13</sub> with the presence of uncapped  $\beta$ -NaSn<sub>12</sub>.<sup>9</sup> This result is indicated in Figure 3; the isomers that are circled in bold are the isomers that were observed with this synthesis strategy. The computational results indicate that single-capped  $\gamma$ -NaSn<sub>13</sub> is more unstable than uncapped  $\beta$ -NaSn<sub>12</sub> by 33.8 kcal mol<sup>-1</sup> and uncapped  $\gamma$ -NaSn<sub>12</sub> by 23.8 kcal mol<sup>-1</sup>. The cap on  $\gamma$ -NaSn<sub>13</sub> yields a short Sn-Sn distance of 3.15 Å. between the cap and the nearest tin, which might destabilize the single-capped  $\gamma$ -NaSn<sub>13</sub> by repulsion, compared to the uncapped  $\gamma$ -NaSn<sub>12</sub>.<sup>9</sup> However, the uncapped  $\gamma$ -NaSn<sub>12</sub> is not observed. One analysis of these values is that a  $\Delta G_{\text{aq}}$  of 23.8 kcal mol<sup>-1</sup> between a capped and uncapped system is in fact sufficient to prevent the respective uncapped system from forming.

**Table 1. Hydrolysis Gibbs free energy (kcal mol<sup>-1</sup>) and HOMO-LUMO gap (eV) of uncapped and capped Na-Sn clusters.**

Cluster	Hydrolysis Gibbs Free Energy (kcal mol <sup>-1</sup> )	HOMO-LUMO gap (eV)
$\varepsilon$ -NaSn <sub>12</sub> <sup>1+</sup>	386.6	5.87
$\alpha$ -NaSn <sub>13</sub> <sup>1+</sup>	369.7	5.17
$\beta$ -NaSn <sub>13</sub> <sup>1+</sup>	364.9	5.28
$\gamma$ -NaSn <sub>13</sub> <sup>1+</sup>	361.2	5.80
$\delta$ -NaSn <sub>12</sub> <sup>1+</sup>	347.3	6.09
$\alpha$ -NaSn <sub>12</sub> <sup>1+</sup>	342.7	6.20
$\gamma$ -NaSn <sub>12</sub> <sup>1+</sup>	337.4	5.91
$\beta$ -NaSn <sub>12</sub> <sup>1+</sup>	327.4	6.24
$\gamma$ -NaSn <sub>14</sub>	272.3	6.04

Synthesis strategy IV performed by *Zhu et al.* in 2019 produced double-capped  $\gamma$ -NaSn<sub>14</sub>.<sup>10</sup> Authors were able to use borate ligands to stabilize the two capping butyltin, which in turn prevented isomerization in solution.<sup>10</sup> It is possible that a more symmetric structure with two caps rather than one allows for a more thermodynamically stable state. The computational results performed in this study indicate that double-capped  $\gamma$ -NaSn<sub>14</sub> is more stable than uncapped  $\beta$ -NaSn<sub>12</sub> by 55.1 kcal mol<sup>-1</sup> and uncapped  $\gamma$ -NaSn<sub>12</sub> by 65.1 kcal mol<sup>-1</sup>, as is shown in Figure 3. It seems that since this double-capped  $\gamma$ -NaSn<sub>14</sub> is more stable than its uncapped counterpart, it dominates in solution. Also, it is possible that since double-capped  $\gamma$ -NaSn<sub>14</sub> is 55.1 kcal mol<sup>-1</sup> more stable than  $\beta$ -NaSn<sub>12</sub>, it prevents uncapped- $\beta$  from forming.

More structures in the Keggin cluster chemical space of Na-Sn need to be synthesized and computationally modeled to truly determine the influence of capping on the thermodynamic stability landscape. What is the energy difference that defines the transition point between forming a mixture of uncapped and capped Keggin clusters, and forming a pure phase? For example, in synthesis strategy III, could uncapped  $\beta$ -NaSn<sub>12</sub> have been prevented from forming if single-capped  $\gamma$ -NaSn<sub>13</sub> had only been 23.8 kcal mol<sup>-1</sup> less stable? Computational tools can be employed to tune the structure of single-capped  $\gamma$ -NaSn<sub>13</sub> slightly to see if there is room for improvement. If a variation of the single-capped  $\gamma$ -NaSn<sub>13</sub> is determined, new syntheses can be designed to create this system. This would remove the need to double-cap the structure, and thus maintain simplicity of the structure and a promising photoresist material for EUV lithography. It should be noted that these energy differences are specific to the level of theory, including the implicit solvation, employed in the computational investigation.

## 5. Conclusions

The understanding of the fundamental lithographic mechanisms at play during exposure of a Na-Sn Keggin photoresist, can be improved first by exploring the tunability of this Na-Sn Keggin system. Computational results provided vital insight towards understanding the nature of this unique system that favors the lower symmetry Keggin isomers,  $\beta$  and  $\gamma$ . The successful collaborative accumulation of computational and experimental results confirmed that the Sn-Keggin clusters represent the only Keggin ion family to this date that favors these lower symmetry isomers. To prevent a mixture of isomers, strategic capping proved to be successful when the hydrolysis Gibbs free energy differences were large enough. Future work will focus on further probing this Sn-Keggin system's possible capping combinations and changing the central heteroatom.

## 6. Acknowledgements

The authors gratefully acknowledge the support of the National Science Foundation, Center for Chemical Innovation, grant CHE-1606982.

## 7. References

- [1] "EUV Lithography Finally Ready For Chip Manufacturing - IEEE Spectrum.", <<https://spectrum.ieee.org/semiconductors/nanotechnology/euv-lithography-finally-ready-for-chipmanufacturing>> (10 September 2019).
- [2] Frederick, R. T., Diulus, J. T., Hutchison, D. C., Olsen, M. R., Lyubinetzky, I., Nyman, M., and Herman, G. S., "Surface characterization of tin-based inorganic EUV resists," *Advances in Patterning Materials and Processes XXXV*, C. K. Hohle and R. Gronheid, Eds., 6, SPIE (2018).
- [3] Passarelli, J., Murphy, M., Del Re, R., Sortland, M., Dousharm, L., Vockenhuber, M., Ekinci, Y., Neisser, M., Freedman, D. A., et al., "High-sensitivity molecular organometallic resist for EUV (MORE)," *Advances in Patterning Materials and Processes XXXII 9425*, T. I. Wallow and C. K. Hohle, Eds., 94250T, SPIE (2015).
- [4] Cardineau, B., Del Re, R., Al-Mashat, H., Marnell, M., Vockenhuber, M., Ekinci, Y., Sarma, C., Neisser, M., Freedman, D. A., et al., "EUV resists based on tin-oxo clusters," *Advances in Patterning Materials and Processes XXXI 9051*, T. I. Wallow and C. K. Hohle, Eds., 90511B, SPIE (2014).
- [5] Saha, S., Park, D.-H., Hutchison, D. C., Olsen, M. R., Zakharov, L. N., Marsh, D., Goberna-Ferrón, S., Frederick, R. T., Diulus, J. T., et al., "Alkyltin keggin clusters templated by sodium," *Angew. Chem. Int. Ed. Engl.* 56(34), 10140-10144 (2017).
- [6] Li, M., Manichev, V., Garfunkel, E. L., Gustafsson, T., Nyman, M., Hutchison, D., Feldman, L. C., and Yu, F., "Novel Sn-based photoresist for high aspect ratio patterning," *Advances in Patterning Materials and Processes XXXV*, C. K. Hohle and R. Gronheid, Eds., 19, SPIE (2018).
- [7] Closser, K. D., Ogletree, D. F., Naulleau, P., and Prendergast, D., "The importance of inner-shell electronic structure for enhancing the EUV absorption of photoresist materials.," *J. Chem. Phys.* 146(16), 164106 (2017).
- [8] Sharps, M. C., Frederick, R. T., Javitz, M. L., Herman, G. S., Johnson, D. W., and Hutchison, J. E., "Organotin Carboxylate Reagents for Nanopatterning: Chemical Transformations during Direct-Write Electron Beam Processes," *Chem. Mater.* (2019).

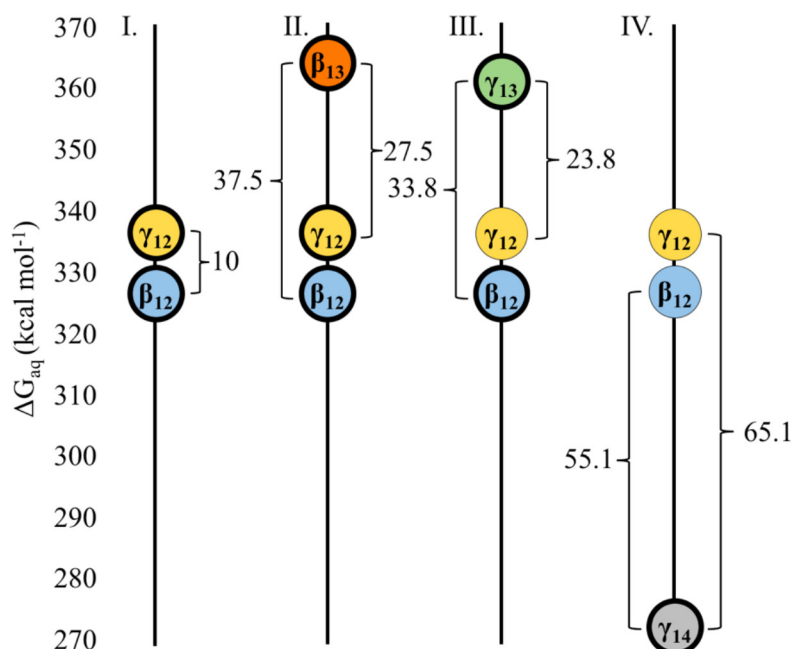


Figure 3. Four synthesis strategies (I, II, III, IV) and their experimentally observed results (bold-circled isomers). Hydrolysis Gibbs free energies of all relevant isomers are included. Blue =  $\beta$ - $\text{NaSn}_{12}$ , Yellow =  $\gamma$ - $\text{NaSn}_{12}$ , Red =  $\beta$ - $\text{NaSn}_{13}$ , Green =  $\gamma$ - $\text{NaSn}_{13}$ , Gray =  $\gamma$ - $\text{NaSn}_{14}$ .

- [9] Hutchison, D. C., Stern, R. D., Olsen, M. R., Zakharov, L. N., Persson, K. A., and Nyman, M., "Alkyltin clusters: the less symmetric Keggin isomers," *Dalton Trans.* 47(29), 9804–9813 (2018).
- [10] Zhu, Y., Olsen, M. R., Nyman, M., Zhang, L., and Zhang, J., "Stabilizing  $\gamma$ -Alkyltin-Oxo Keggin Ions by Borate Functionalization," *Inorg. Chem.* 58(7), 4534–4539 (2019).
- [11] Keggin, J. F., "Structure of the Molecule of 12-Phosphotungstic Acid," *Nature* 131(3321), 908–909 (1933).
- [12] Zhang, F.-Q., Guan, W., Zhang, Y.-T., Xu, M.-T., Li, J., and Su, Z.-M., "On the origin of the inverted stability order of the reverse-Keggin [(MnO<sub>4</sub>)(CH<sub>3</sub>)<sub>12</sub>Sb<sub>12</sub>O<sub>24</sub>]<sub>6</sub>⁻: a DFT study of alpha, beta, gamma, delta, and epsilon isomers," *Inorg. Chem.* 49(12), 5472–5481 (2010).
- [13] Wills, L. A., Qu, X., Chang, I.-Y., Mustard, T. J. L., Keszler, D. A., Persson, K. A., and Cheong, P. H.-Y., "Group additivity-Pourbaix diagrams advocate thermodynamically stable nanoscale clusters in aqueous environments," *Nat. Commun.* 8, 15852 (2017).
- [14] Casasnovas, R., Ortega-Castro, J., Frau, J., Donoso, J., and Muñoz, F., "Theoretical  $pK_a$  calculations with continuum model solvents, alternative protocols to thermodynamic cycles," *Int. J. Quantum Chem.* 114(20), 1350–1363 (2014).
- [15] Sundstrom, E. J., Yang, X., Thoi, V. S., Karunadasa, H. I., Chang, C. J., Long, J. R., and Head-Gordon, M., "Computational and experimental study of the mechanism of hydrogen generation from water by a molecular molybdenum-oxo electrocatalyst," *J. Am. Chem. Soc.* 134(11), 5233–5242 (2012).
- [16] Zhang, L., Dembowski, M., Arteaga, A., Hickam, S., Martin, N. P., Zakharov, L. N., Nyman, M., and Burns, P. C., "Energetic trends in monomer building blocks for uranyl peroxide clusters," *Inorg. Chem.* 58(1), 439–445 (2019).
- [17] Becke, A. D., "Density-functional thermochemistry. III. The role of exact exchange," *J. Chem. Phys.* 98(7), 5648 (1993).
- [18] Hariharan, P. C. and Pople, J. A., "The influence of polarization functions on molecular orbital hydrogenation energies," *Theor. Chim. Acta* 28(3), 213–222 (1973).
- [19] Wadt, W. R. and Hay, P. J., "Ab initio effective core potentials for molecular calculations. Potentials for main group elements Na to Bi," *J. Chem. Phys.* 82(1), 284–298 (1985).
- [20] Marenich, A. V., Cramer, C. J., and Truhlar, D. G., "Universal solvation model based on solute electron density and on a continuum model of the solvent defined by the bulk dielectric constant and atomic surface tensions," *J. Phys. Chem. B* 113(18), 6378–6396 (2009).
- [21] Krishnan, R., Binkley, J. S., Seeger, R., Pople, J. A., "Self-consistent molecular orbital methods. XX. A basis set for correlated wave functions," *J. Chem. Phys.* 72(1), 650 (1980).
- [22] López, X., Maestre, J. M., Bo, C., and Poblet, J.-M., "Electronic Properties of Polyoxometalates: A DFT Study of  $\alpha / \beta$  -[XM<sub>12</sub>O<sub>40</sub>]<sup>n</sup> - Relative Stability (M = W, Mo and X a Main Group Element)," *J. Am. Chem. Soc.* 123(39), 9571–9576 (2001).
- [23] Armstrong, C. R., Casey, W. H., and Navrotsky, A., "Energetics of Al<sub>13</sub> Keggin cluster compounds," *Proc. Natl. Acad. Sci. USA* 108(36), 14775–14779 (2011).
- [24] Wang, W., Fullmer, L. B., Bandeira, N. A. G., Goberna-Ferrón, S., Zakharov, L. N., Bo, C., Keszler, D. A., and Nyman, M., "Crystallizing elusive chromium polycations," *Chem* 1(6), 887–901 (2016).
- [25] Wang, W., Amiri, M., Kozma, K., Lu, J., Zakharov, L. N., and Nyman, M., "Reaction Pathway to the Only Open-Shell Transition-Metal Keggin Ion without Organic Ligand," *Eur J Inorg Chem* 2018(42), 4638–4642 (2018).
- [26] López, X. and Poblet, J. M., "DFT study on the five isomers of PW(12)O(40)(3)(-): relative stabilization upon reduction," *Inorg. Chem.* 43(22), 6863–6865 (2004).
- [27] López, X., Carb., J. J., Bo, C., and Poblet, J. M., "Structure, properties and reactivity of polyoxometalates: a theoretical perspective," *Chem. Soc. Rev.* 41(22), 7537–7571 (2012).



## Sponsorship Opportunities

Sign up now for the best sponsorship opportunities

### Photomask Technology + EUV Lithography 2020

Contact: Melissa Valum  
Tel: +1 360 685 5596; [melissav@spie.org](mailto:melissav@spie.org)

### Advanced Lithography 2021

Contact: Teresa Roles-Meier  
Tel: +1 360 685 5445; [teresar@spie.org](mailto:teresar@spie.org)

## Advertise in the BACUS News!

The BACUS Newsletter is the premier publication serving the photomask industry. For information on how to advertise, contact:

Melissa Valum  
Tel: +1 360 685 5596  
[melissav@spie.org](mailto:melissav@spie.org)

## BACUS Corporate Members

Acuphase Inc.  
American Coating Technologies LLC  
AMETEK Precitech, Inc.  
Berliner Glas KGaA Herbert Kubatz GmbH & Co.  
FUJIFILM Electronic Materials U.S.A., Inc.  
Gudeng Precision Industrial Co., Ltd.  
Halocarbon Products  
HamaTech APE GmbH & Co. KG  
Hitachi High Technologies America, Inc.  
JEOL USA Inc.  
Mentor Graphics Corp.  
Molecular Imprints, Inc.  
Panavision Federal Systems, LLC  
Profilcolore Srl  
Raytheon ELCAN Optical Technologies  
XYALIS

# Industry Briefs

## ■ Key Drivers In New Chip Industry Outlook

### Ed Sperling

How well the semiconductor industry fares over the next 12 to 24 months depends upon the evolution of a virus. That alone will determine the correct model for an economic rebound — V, U, extended U, or maybe even a double U.

But what's also becoming clear is those models don't apply uniformly to all sectors of the semiconductor industry. While the entire industry is and will continue to be affected, some areas have seen positive growth. For example, consumer electronics sales have boomed since the start of shutdowns, especially in the area of webcams and gaming. Automotive sales, meanwhile, have slumped, dragging down semiconductor sales in that market. Likewise, the planned rollout for 5G has been pushed out at varying levels across multiple regions, offsetting predictions about equipment sales.

Current models of growth in semiconductors range from +6% in 2020 to -28% in some segments, depending upon the length of the impact, the liquidity of markets over that time, how many more shutdowns there will be, and how quickly consumer confidence rebounds. None of this is clear at this point, and no one is quite certain when it will be.

<https://semiengineering.com/key-drivers-in-new-chip-industry-outlook/>

## ■ TSMC confirms investment talks with U.S. but no concrete plans yet

Taiwan Semiconductor Manufacturing Co. (TSMC), the world's largest contract chipmaker, confirmed a report that it has entered into talks with the U.S. Department of Commerce (DOC) on building a plant in the United States. It stressed, however, that it has no concrete plans for a potential investment at present.

TSMC said the company continues to evaluate any possibility of building a plant outside Taiwan, and the U.S. is just one of the options. Any overseas investment plan would take into account clients' needs and several other factors such as the state of the global economy, the supply chain, its workforce and production costs.

Beyond TSMC, the DOC has also been in talks with American semiconductor giant Intel Corp. on the possibility of building a chip plant there, according to the Wall Street Journal.

<https://focustaiwan.tw/business/202005110016>

## ■ SMIC Aims to Raise More Than \$3B for Expansion

### Alan Patterson

<https://www.eetimes.com/smhc-aims-to-raise-more-than-3b-for-expansion/>

Semiconductor Manufacturing International Corp. (SMIC), based in Shanghai, aims to sell new shares to raise more than \$3 billion for investment in expansion.

The board of China's biggest foundry earlier this month approved a proposal to issue 1.69 million new shares on China's Sci-Tech Innovation Board, also known as the STAR market, for technology companies. SMIC said 40 percent of the money raised will be used for its "12-Inch SNI Project"; 20 percent for R&D on advanced and mature technology; and the rest for the replenishment of working capital. The company has been seeking alternative funding sources after it delisted from the New York Stock Exchange last year amid increasing restrictions by the U.S. against Chinese tech companies. Analysts believe that access to advanced manufacturing equipment is the biggest challenge for SMIC in its efforts to expand.

Huawei may lose access to Taiwan Semiconductor Manufacturing Co.'s most advanced production technology in the future, the report said. The U.S. government has been trying to restrict TSMC's sales to Huawei, one of the world's leading makers of 5G equipment. Huawei may try to redirect some chip orders to SMIC, but it will be impossible for SMIC to meet these expectations if the company does not have U.S. chipmaking equipment, according to the report.

Huawei's chipmaking subsidiary, HiSilicon, is using TSMC's 7nm technology for production of its Kirin processors. SMIC lags three generations behind TSMC at the 14nm node. The United States has even blocked SMIC from buying EUV lithography equipment from ASML of the Netherlands, which is key to upgrading the Chinese company's production technology.

<https://semiengineering.com/metrology-challenges-for-gate-all-around/>

# Join the premier professional organization for mask makers and mask users!

## About the BACUS Group

Founded in 1980 by a group of chrome blank users wanting a single voice to interact with suppliers, BACUS has grown to become the largest and most widely known forum for the exchange of technical information of interest to photomask and reticle makers. BACUS joined SPIE in January of 1991 to expand the exchange of information with mask makers around the world.

The group sponsors an informative monthly meeting and newsletter, BACUS News. The BACUS annual Photomask Technology Symposium covers photomask technology, photomask processes, lithography, materials and resists, phase shift masks, inspection and repair, metrology, and quality and manufacturing management.

### Individual Membership Benefits include:

- Subscription to BACUS News (monthly)
- Eligibility to hold office on BACUS Steering Committee

[spie.org/bacushome](http://spie.org/bacushome)

### Corporate Membership Benefits include:

- 3-10 Voting Members in the SPIE General Membership, depending on tier level
- Subscription to BACUS News (monthly)
- One online SPIE Journal Subscription
- Listed as a Corporate Member in the BACUS Monthly Newsletter

[spie.org/bacushome](http://spie.org/bacushome)

## C A L E N D A R

### 2020

#### **The 36th European Mask and Lithography Conference, EMLC 2020**

22-24 June 2020  
Leuven, Belgium

#### **SPIE Photomask Technology + EUV Lithography**

20-24 September 2020  
Monterey Conference Center and  
Monterey Marriott  
Monterey, California, USA

### 2021

#### **SPIE Advanced Lithography**

21-25 February 2021  
San Jose, California, USA  
[www.spie.org/al](http://www.spie.org/al)

#### **Photomask Japan**

26-28 April 2021  
Yokohama, Kanagawa, Japan  
[www.photomask-japan.org](http://www.photomask-japan.org)

SPIE is the international society for optics and photonics, an educational not-for-profit organization founded in 1955 to advance light-based science and technology. The Society serves more than 255,000 constituents from 183 countries, offering conferences and their published proceedings, continuing education, books, journals, and the SPIE Digital Library in support of interdisciplinary information exchange, professional networking, and patent precedent. In 2019, SPIE provided more than \$5 million in community support including scholarships and awards, outreach and advocacy programs, travel grants, public policy, and educational resources. [spie.org](http://spie.org)

### **SPIE.**

International Headquarters  
P.O. Box 10, Bellingham, WA 98227-0010 USA  
Tel: +1 360 676 3290  
Fax: +1 360 647 1445  
[help@spie.org](mailto:help@spie.org) • [spie.org](http://spie.org)

Shipping Address  
1000 20th St., Bellingham, WA 98225-6705 USA

#### **Managed by SPIE Europe**

2 Alexandra Gate, Ffordd Pengam, Cardiff,  
CF24 2SA, UK  
Tel: +44 29 2089 4747  
Fax: +44 29 2089 4750  
[spieeurope@spieeurope.org](mailto:spieeurope@spieeurope.org) • [spieeurope.org](http://spieeurope.org)

You are invited to submit events of interest for this calendar. Please send to [lindad@spie.org](mailto:lindad@spie.org).